Electron refluxing and K-shell line emission from Ti foils irradiated with sub-picosecond laser pulses at 527nm

Nersisyan, G., Riley, D., Lewis, C., Nedanovska, E., Dzelzainis, T., Nicholl, R., Makita, M., McKeever, K., White, S., Kettle, B., & Williams, G. (2012). Electron refluxing and K-shell line emission from Ti foils irradiated with sub-picosecond laser pulses at 527nm. *Physical Review E*, *85*(5), [056415]. https://doi.org/10.1103/PhysRevE.85.056415

Published in:
Physical Review E

Document Version:
Peer reviewed version

Electron refluxing and K-shell line emission from Ti foils irradiated with sub-picosecond laser pulses at 527nm

G Nersisyan, M Makita, K McKeever, T Dzelzainis, S White,
E Nedanovska, B Kettle, R Nicholl, G Williams, D Riley and CLS Lewis
Centre for Plasma Physics, School of Mathematics and Physics,
Queen's University Belfast, University Road, Belfast BT7 1NN, UK[*]

(Dated: May 9, 2012)

Abstract

We present data on emission of K-shell radiation from Ti foils irradiated with sub-picosecond pulses of second harmonic radiation (527nm) from the TARANIS laser system at intensities of up to 10^{18}Wcm^{-2}. The data is used to demonstrate that a resonance absorption type mechanism is responsible for absorption of the laser light and to estimate fast electron temperatures of 30-60keV that are in broad agreement with expectation from models of absorption for a steep density gradient. Data taken with resin-backed targets are used to demonstrate clear evidence of electron refluxing even at the modest fast electron temperatures inferred.

PACS numbers: 52.38.Ph, 52.38.Dx, 52.70.La

[*]Corresponding author: d.riley@qub.ac.uk

I. INTRODUCTION

Over the years there have been several studies of K-α e.g. [1–8] and thermal X-ray line e.g. [9, 10] emission from laser plasmas. Some of these studies were aimed at understanding fast electron (alternatively called hot electron) propagation in solids under intense laser irradiation [11], whilst others were aimed at developing sources of x-rays for other purposes, such as absorption spectroscopy, radiography or X-ray scattering [12]. Previously published data has covered both fundamental and second harmonic laser radiation for femto-second laser systems [3]. For pulses of 60ps and longer, both first and second harmonic have been studied [9, 10]. For nanosecond pulses yields of thermal X-rays for third harmonic have been measured [13].

In this paper we address three points. Firstly, we present absolute measurements of Ti K-α (2.75Å) photon yields, for source development purposes. The laser irradiation conditions investigated occupy, from the point of view of K-α yield measurement, a relatively unexplored combination of wavelength and pulse duration parameter space; that is at 0.8 ps duration with high contrast second harmonic (527nm) light. Secondly, we compare the yield of K-α radiation with the yield of the He-α line (He-like $1s^2 - 1s2p^1$P and satellites at 2.61-2.75Å) for pulse durations intermediate between the fs [14] and sub-ns regimes [9, 15]. Finally, we investigate, experimentally, the role of refluxing of fast electrons in determining the yield of K-α radiation. In the course of this investigation, we measure the temperature of the fast electron population generated principally by a resonance absorption type mechanism and show that a simple model for K-α emission is consistent with the measurements and the interpretation.

II. EXPERIMENT

The experiment was carried out with the second harmonic of the laser pulses delivered by the high power laser system, TARANIS [16] situated at Queen's University Belfast. This Ti:Sapphire-Nd:Glass CPA laser can provide pulses of 800 fs duration and of up to 15 J energy after the compressor at 1053nm wavelength. However, in this work the energy of the laser was kept low in order to improve the focal spot quality. The intensity contrast of the laser at 1-2 ns before the main pulse was measured by a fast photodiode (rise time 200ps)

yielding contrast of about 10^7 for ASE. The pre-pulse activity consisted of a few, picosecond duration, pre-pulses at up to ∼3ns ahead of the main pulse with energy contrast of 10^4 for the 1053nm beam.

The pulses of the second harmonic at 527 nm wavelength were generated by a 2 mm thick KDP (Type I) crystal. The unconverted infrared emission was rejected by two flat mirrors and an off-axis parabola (OAP) with dielectric coatings of high reflectivity optimized for the second harmonic. These mirrors delivered the second harmonic pulses to the target. The p-polarized second harmonic emission was focused by the F/3.3 OAP to a focal spot of 12μm full-width-at-half-maximum (FWHM) in diameter containing 50% of the energy. The size of the focal spot was inferred from preliminary shots in which a 4.6m focal length lens was used to focus the full beam down onto a CCD camera after reflection of three high quality optical flats to reduce intensity to a level where appropriate filtering could be used to make measurements. In figure 1 we can see a typical focal spot profile taken with the long focal length lens. We note that there is a degree of astigmatism in the distribution and we refer to this later in the interpretation of the data. In this experiment we used second harmonic energies up to 2.5J with much of the data taken with ∼1J on target with an intensity at 45° incidence of $\sim 4 \times 10^{17}$ Wcm^{-2}, where the average irradiance is defined taking the energy and dividing by the full-width-at-half-maximum (FWHM) duration and by a focal spot area defined by the FWHM diameter of the spot. Variation of the focused intensity down to about 3×10^{15} Wcm^{-2} was achieved by defocusing the beam on the target by up to 1mm. The transmission of the beamline beyond the crystal, for the unconverted fundamental was measured to be 7.8×10^{-3} %, resulting in an ASE pre-pulse intensity, at 1053 nm, on target of $< 10^7$ Wcm^{-2}. For pre-pulses the focused energy was estimated to be $<$ 50nJ per pulse with focused intensity estimated at $< 10^{10}$ Wcm^{-2} in a picosecond pulse. The resulting fluence of < 0.05Jcm^{-2} would then be below the ablation threshold.

The K-shell emission from laser-heated thin foils of Ti was monitored with two spectrometers, each consisting of a Bragg crystal coupled to a CCD detector. These were fitted with cylindrically curved (R=50mm) highly oriented pyrolytic graphite (HOPG) crystals (2d=6.708Å) operating in the von-Hamos configuration. One of these detectors was placed to view the laser irradiated (front) side of the foil approximately along the normal to the foil surface, when the laser was incident at 45° on the target. For the same target position, the second spectrometer was placed to view the un-irradiated (rear) side of the target at

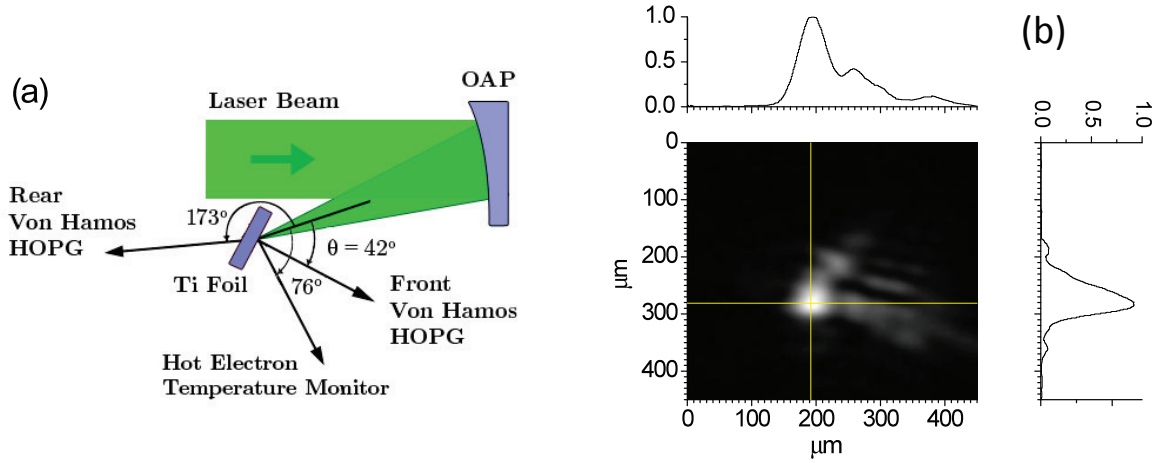

FIG. 1: (Color online) (a) Schematic of the experimental layout. Angles shown for the diagnostics are relative to the laser axis and are fixed. (b) A typical focal spot measured at full energy in second harmonic with a 4.6 m lens after picking of a small fraction of the beam energy with flat plates. For the OAP the scaled FWHM containing 50% of the energy was 12 μm. The scale in the image is the same as in the line-outs.

at 35° from the normal. We can see the layout schematically in figure 1. The integrated reflectivity of the HOPG crystals was determined to ±15% in a separate experiment by comparison of spectra with a single hit CCD detection system using low energy shots. This calibration work will be described in a separate paper.

In order to get an estimate of the fast electron temperature, we also fielded a simple instrument consisting of an array of five filters (with thicknesses ranging from 50-400 μm of Pb) with an image plate as the detector. The principle of the instrument is that we assume the bremsstrahlung emission generated from fast electrons has a spectral shape given by $I(E, T_h) \sim exp(-E/kT_h)$ where T_h is the fast electron temperature, k is the Boltzmann constant and E is the photon energy. By accounting for the response of the image plate (Fuji MS type) to hard X-rays [17] and the filter transmission [18], we can find a value for fast electron temperature by comparing the ratio of signal levels in the different spectral channels. The filter array and IP sat outside the chamber and a 300 μm plastic window allowed X-rays to pass. A collimating tube covered in lead (thickness 1mm) and with a slot at the front ensured that the instrument viewed only X-rays from the region of the target and helped to reduce the plasma striking the window and causing fluorescence. The window also prevented fast electrons from reaching the Pb filters. The background that did appear

on the image plate was smooth and quite uniform. It showed a clear and reproducible fall with distance as we moved the image plate back from the filters by up to 16cm and was relatively simple to remove in analysis. For the range of temperatures we observe below, the data is reliable for 3-4 filters, the thickest showing little signal. Sensitivity analysis carried out by varying the background subtraction allowed error bars to be determined.

In the next section, we present the data relevant to the first two points we address -i.e. fractional yields of K-α/He-α radiation and the fast electron temperature. In the following section we present modelling in conjunction with data relevant to the issues of fast electron reflux.

III. EXPERIMENTAL RESULTS

In figure 2 we show a typical spectrum from the front HOPG spectrometer. We can see the K-α and K-β lines. We also see H-like and He-like Ti emission lines and evidence of inner shell emission from a series of ionisation stages. The ratio of the He-α and Lyman-α lines indicates T_e >2keV for the "thermal" background temperature [19]. This should be a lower limit since, even if we assume heat flows from critical density up to $N_e \sim 10^{23}$ cm^{-3}, we would expect the timescale for ionisation from He-like to H-like ground states to be of order 10 ps for T_e=2 keV. A fast electron population at 30 keV would have an ionisation rate more than 20 times faster but the effect of this would depend on the fast electron density as a fraction of the total and we do not have a good estimate of this.

In figure 3, for 45° incidence and p-polarisation, we see the absolute fractional yields of K-α photons as a function of defocus distance for three thicknesses of Ti foils, for both the front and rear spectrometers. Each point is an average of several shots and the error bars are standard deviations from the mean. The fractional yield is defined as the energy emitted in K-α photons into 4π sr divided by the incident laser energy. For our purposes, the calculations take the spectrometer measurements and extrapolate assuming isotropic emission. Naturally, in reality, emission in some directions will be re-absorbed more than others and this is reflected in the lower yields seen for the rear spectrometer with thick foils. The effect of re-absorption is taken into account in our simulations when we make comparisons to data below. Notice that the ratio of approximately 1:1 for front and rear emission in the tight focus case for 10 μm foils is as expected, due to the approximately 20

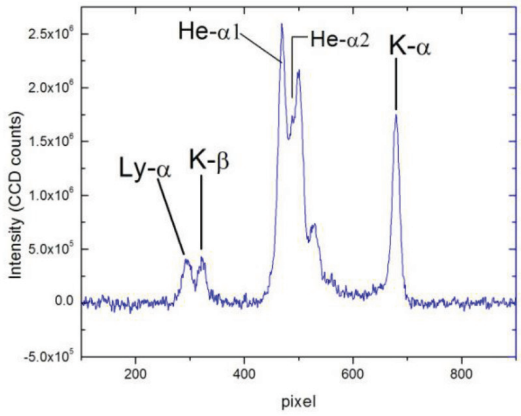

FIG. 2: (Color online)Typical spectrum at tight focus, showing the K-α and K-β lines as well as thermal emission from H-like and He-like ions. The ratio of He-α to Lyman-α is used to infer an electron temperature of T_e >2keV (see text)

μm absorption length of K-α photons combined with penetration of electrons into the foil. This also gives confidence in the relative calibration of the crystals. In the 25 and 50 μm foil cases, the effect of increased electron penetration in increasing the signal from the foil rear, at tight focus, is clear. An important feature is that, in all three cases, there seems to be a minimum at 50 μm away from where we determined best focus to be. The depth of this dip increases only slightly for thicker targets, suggesting that this is not, in fact, a result of the deep penetration of electrons into the foils but may be linked to a change in the efficiency of converting laser energy to fast electron energy, close to best focus. This may be a result of the astigmatic focal spot, where, as seen above, a low intensity halo contains half the energy at tight focus. It is also possible that at the lower intensity away from best focus, the density scale-length is slightly more optimised for absorption at 45° than for the tight focus case. The scale-length and absorption mechanism are discussed below.

In figure 4, we can see the normalised yield of K-α photons as a function of angle at tight focus for 50 μm foils. Again, the data is averaged over 4-5 shots and the error bars represent standard deviations of the yield. By assuming that the yield is proportional to the absorption, we have estimated the plasma density scale-length of the plasma by fitting the data to a simple resonance absorption model [20]. A least squares best fit gives a scale-length of L=$0.18 \pm 0.02\mu$m. This means that $L/\lambda \approx 0.34$ and since $v_{osc}/\omega_0 \approx 0.024\mu\text{m} < L$, then we expect to be in the resonance absorption regime rather than the vacuum heating [21, 22]

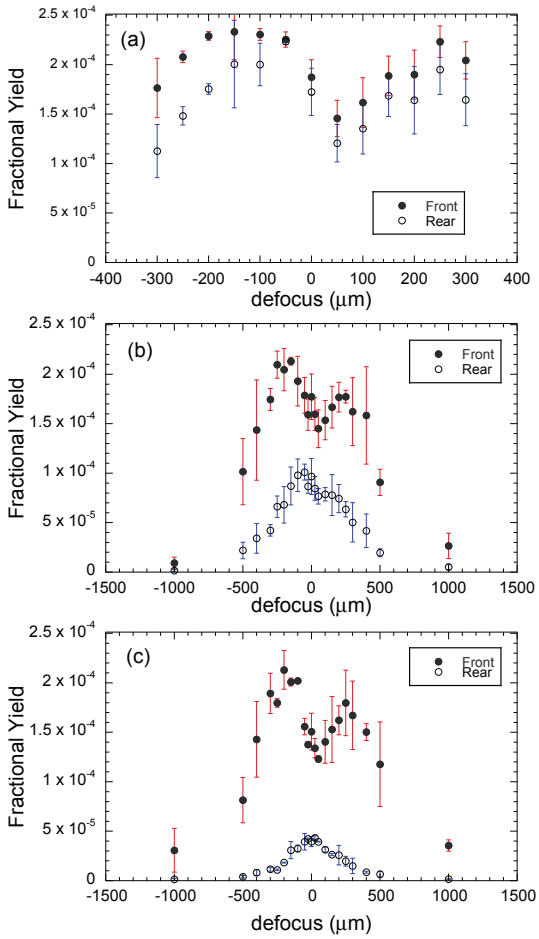

FIG. 3: (Color online) K-α fractional yields for front (solid disks) and rear (open circles) spectrometers as a function of defocus for a) 10 μm, b) 25μm and c) 50μm Ti foils. Positive defocus means the focus is in front of the target. Error bars are standard deviations. Note the different spatial scale for the 10μm case.

regime which would apply at shorter scale-length. For the intensities used, ponderomotive steepening may be important in setting the scale-length. We expect the pressure associated with the laser to be ≈35 Mbar, equivalent to a thermal temperature of over 5 keV at critical density. We make a more sophisticated estimate of scale-length in the modelling section below after describing our K-α generation model and the measurement of fast electron temperature, but the result is as for the simple fitting in figure 4.

In figure 5 we can see the fast electron temperature results from the filter array system. At tight focus, the occasional shot can go to nearly 50 keV but quite consistently the temperature is ∼30 ± 5 keV. Defocusing to about 200 μm (and thus increasing focal spot

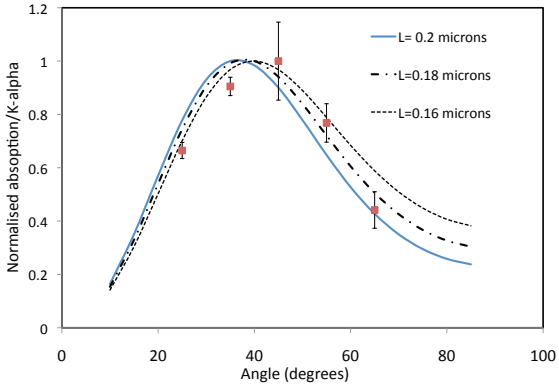

FIG. 4: (Color online) Comparison of K-α yield with normalised absorption for resonance absorption. Using a normalised plot we can estimate the scale-length independently of absorbed laser energy.

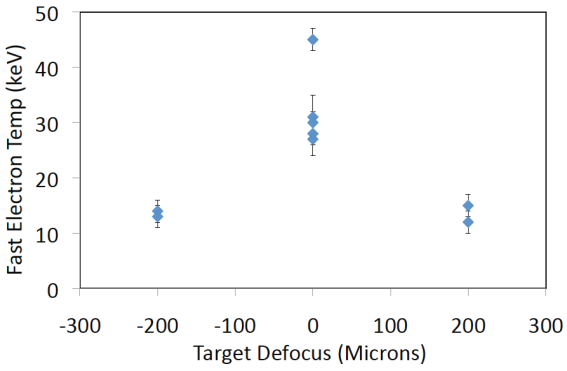

FIG. 5: (Color online) Fast electron temperature as determined by the filter array system.

size by $\sim$5) dropped the estimated fast electron temperature by about a factor of 3, which agrees quite well with a scaling of temperature with $I^{1/3}$ [28,29].

For the He-α line, we expect the emission to depend on the temperature of the "thermal" plasma created around the critical density. In figure 6, we can see the yield as a function of defocus for the case of 50 μm foils. In fact the results are similar for all thicknesses of foil. As we can see from figure 6, the He-like emission generally drops off with defocus more rapidly than the K-α radiation and the maximum yield is comparable to K-α, as for the case of shorter pulses [14] and in contrast to the long pulse case where thermal emission is often at least an order of magnitude more efficient [9]. The large variation in error bars (which are standard deviations as for the K-α case) across the data is a result of statistical variation in yield from shot to shot.

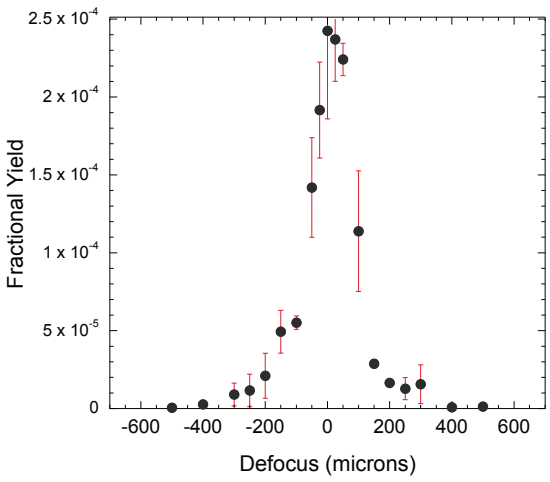

FIG. 6: (Color online) He-α yield as a function of defocus for a 50 μm foil. The overall yield is comparable to the K-α.

IV. MODELLING AND ANALYSIS

Modelling of the complete experiment is in principle complex. A hydro-dynamic code can model the laser plasma interaction including resonance absorption. However, usually non-local heat flow and fast electron transport are not included. For a particle in cell (PIC) simulation, we can model fast electron generation but we must generally start from a plasma that already has a bulk electron temperature of ~ 1 keV in order to resolve the Debye length. Resistivity of the target is also generally not included. In this experimentally based paper we simply seek to broadly understand the level of K-α generation and the behaviour with target thickness, angle of incidence and whether we view from the front or rear of the foil.

With that in mind, we model the K-α generation using a simple one dimensional model presented in a previous paper [23] and based on a model from other authors [2]. In our simple model we assume that conductivity of the metallic target is such that electric field inhibition is not a factor. We have assigned 112 energy groups to the electron population with numbers in each group according to a single temperature in a 1-dimensional Maxwellian distribution as in [2]. The foil is divided into 100 cells and each group is transported through them losing energy according to a stopping power equation and generating K-shell vacancies according to a cross-section from the literature [24]. The K-α yield is calculated accounting for the fluorescence yield and the angle dependent absorption on the way out of the target.

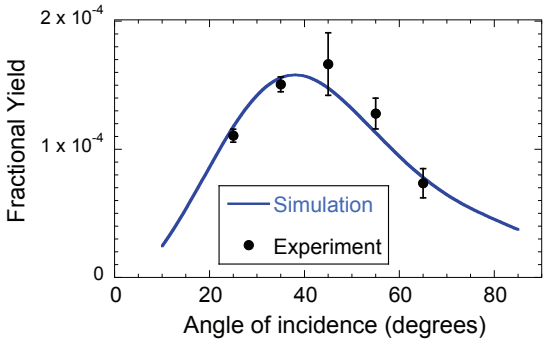

FIG. 7: (Color online) Comparison of K-α fractional yield versus angle for experiment with prediction based on simple modelling as described in text, assuming 23% peak absorption into T_h=30 keV electrons with a scale-length of 0.18 μm.

The most important variable inputs to the code include the fast electron temperature and the fractional absorption into fast electrons.

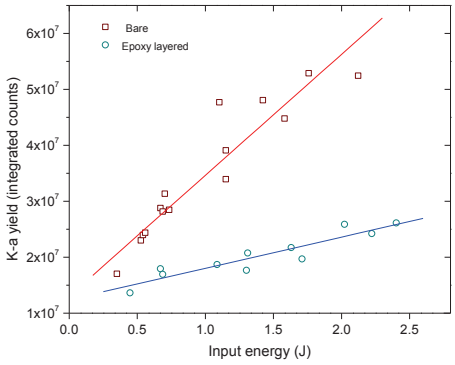

FIG. 8: (Color online) K-alpha signal as a function of incident second harmonic laser energy for resin-backed (blue circles) and bare (red squares) foils of 10 μm thickness.

In figure 4, we assumed absorption was proportional to K-α yield in order to fit a scale-length. With the simple K-α model we can account for variation in yield with temperature and use comparison of absolute and predicted yields for 50 μm foils to fit to both scale-length and peak absorption. In order to account for variation in intensity as angle changes, we assume the experimentally determined value of fast electron temperature at 45° (30 keV) and assume that T_h varies as $I^{1/3}$. Our results are presented in figure 7, where we found that the best fit is for an overall peak absorption of 23±1% of laser energy into fast

electrons with a scale-length of $0.18 \pm 0.02\mu$m in agreement with the simpler derivation of figure 4. In this simulation, we assume that electrons reaching the rear of the foil can reflux back into the target to further contribute to the yield. This issue is discussed and the assumption justified below. In fact varying the expected T_h from 20-60 keV varies the best fit to absorption by only a small amount (23-26%). The absorption fraction calculated here accounts for the whole laser energy. If we assume the low intensity "halo" contributes little to the K-α generation, we would then predict 45-50% absorption in the central hot spot, which is within reasonable bounds for the resonance absorption mechanism. An important

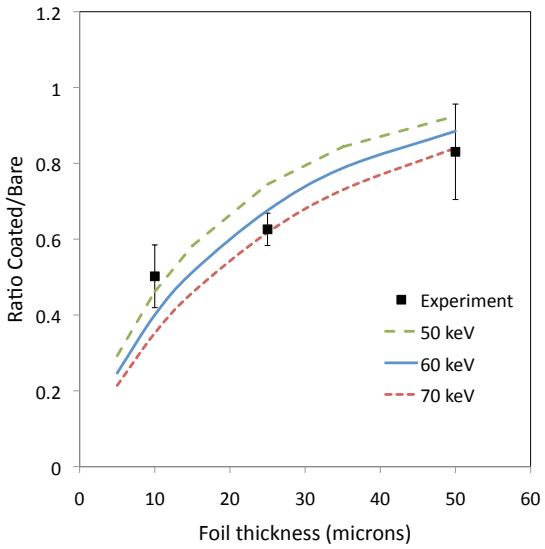

FIG. 9: (Color online) Comparison of experimental K-α yield ratios for coated and bare foils compared to simulation for a range of fast electron temperatures.

issue we also investigated is the role of refluxing in generating K-α yield. We expect this to be dependent primarily on the fast electron temperature. In order to experimentally investigate this, we have carried out further experiments using foils that have been backed by an ≈1mm thick layer of resin (A/epichlorohydrin, $C_{21}H_{25}ClO_5$). The principle is that electrons escaping the rear of the Ti will penetrate the resin and be lost rather than be reflected back into the Ti foil to enhance K-α production. This is similar in design to experiments carried out at the fundamental wavelength by Neumayer *et al* [25]. We coated all three thicknesses of foil with the resin. In order to ensure consistent laser parameters we mounted both coated and uncoated targets on the target drive and alternated shots. The results for the 10 μm foil case can be seen in figure 8 where we have scanned energy on

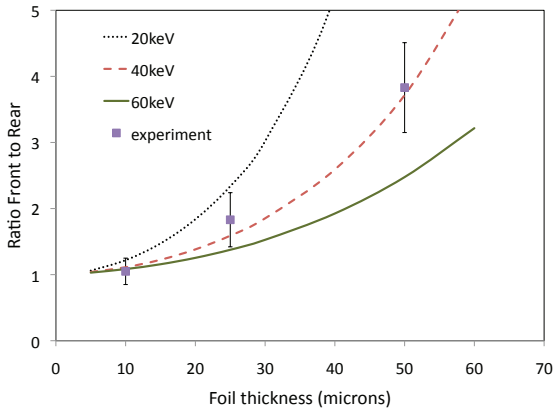

FIG. 10: (Color online) Ratio of K-α emission for the front and rear spectrometers. The solid lines represent simulations and show a best fit of T_h ~40 keV.

target at tight focus. Beyond a certain threshold, we see an almost linear rise with energy for the front spectrometer in both coated and uncoated cases. However, the coated case rises with a different slope and we can see there is clearly a significant contribution from refluxing that increases with energy on target to effectively double the yield. We also see that, at low energy, the slopes seem to converge; evidently, as fast electron temperature drops, refluxing is, as expected, less important. In figure 9 we can see averaged values at peak energy (~1J in this run) for all three thicknesses. What we show in the figure is the ratio of the front surface yields for coated to uncoated targets. Evidently, thickness is important, as might be expected, with only a 20% difference for 50 μm foils compared to a factor of ≈2 for 10 μm foils. What is clear from figure 9, is that refluxing is still an important process even for our relatively modest fast electron temperatures. In figure 9, we compare experimental data to our simple K-α model prediction for the effect of refluxing switched on and off. Using a least squares fit to the data, the best agreement is for temperature of 60 ± 10keV, higher than the filter pack estimate.

A further quantity that is sensitive to the fast electron temperature is the ratio of front to rear emission for uncoated foils. We can see in figure 10 a plot of the averaged ratio at tight focus for all three foil thicknesses. We also see curves predicting the ratio for a range of fast electron temperatures, where a temperature of 40 ± 5 keV seems to best fit the data. We note that for the simulations in figures 9 and 10, we have assumed that electrons reaching the rear of an uncoated foil can reflux back into the foil. This assumption

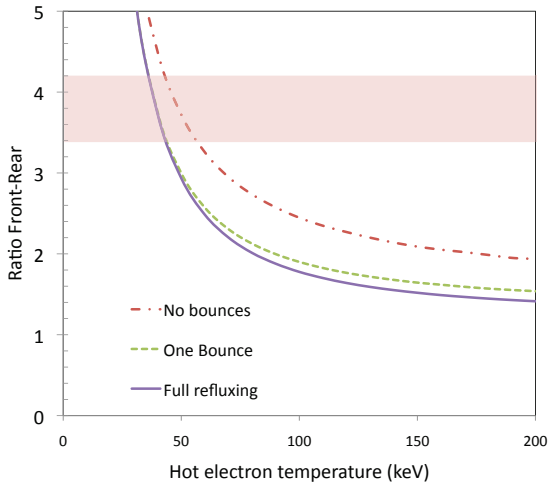

FIG. 11: (Color online) Simulated ratio of front to rear ratio for K-α emission from 50 μm foils, compared to different assumptions about the level of electron refluxing. The red band shows the limits of the error bars for the experimental ratio (3.8±0.4)

is certainly justified from the data in figure 9. However, we need to consider if the refluxing is limited in some way, as this might affect the fast electron temperature that best fits the experimental data. To test this idea, we have run further simulations, as displayed in figure 11. We can see that assuming electrons only bounce once, from the rear surface, makes little difference to the ratio predicted for front to rear emission for the case of 50 μm foils.

There are several scaling laws for fast electron temperature in the literature e.g. [26–28]. As we have shown above, we expect that a resonance absorption type mechanism is dominant. For this mechanism, Kruer and Wilks [27] quote a scaling law $T_h(\mathrm{keV})=10(\mathrm{T}_c I_{15}\lambda^2)^{1/3}$ where T_c is the bulk temperature at critical density in keV, λ is the laser wavelength in microns and I_{15} is the laser intensity in units of 10^{15} Wcm^{-2}. If we take a lower bound for T_c as 2 keV based on the ratio of H-like to He-like emission in figure 2, we estimate T_h= 60 keV. This seems to agree with the data from the refluxing experiment but is higher than the filter pack measurements by about a factor of ≈ 2.

We can note that a different fast electron scaling for short scale-length plasmas Andreev et al [28] has $T_h(\mathrm{keV}) = 8(I_{16}\lambda^2)^{1/3}$ keV and would predict T_h=18 keV. Our experiment suggests a broad 30-60keV range for T_h. In figure 12, we show our three estimates compared to scaling laws from Wilks and Kruer (WK), for Brunel absorption and for the scaling of Andreev. For the WK scaling, we show more than one bulk temperature since our estimate

from the He and H-like lines is only crude. The filter array data at two different focal positions seems to support the scaling of $T_h \propto I^{1/3}$.

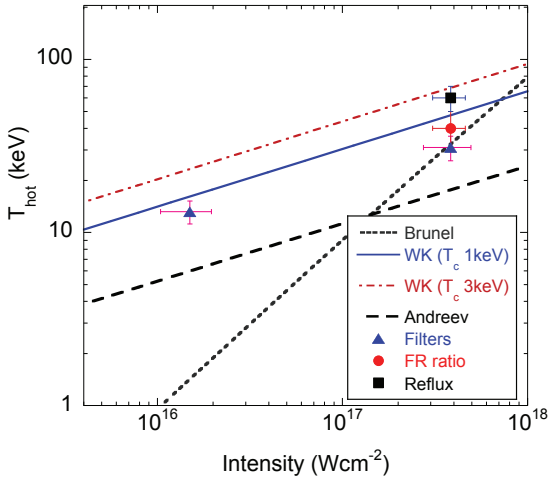

FIG. 12: (Color online) Comparison for the three methods for determining fast electron temperature, at tight focus, with expected temperatures from Brunel [22], Andreev [28] and resonance absorption (WK) [27] with two different estimates of cold plasma temperature spanning the estimate from spectroscopic observation. Data from the hot electron temperature monitor is shown for the focal positions of figure 5. For the experimental data, we have grouped shots and the error bars represent variance of intensity and inferred temperature for both positions.

We can compare our fast electron temperatures to previous work in a similar regime. Yu et al [29] used a similar laser system but with ∼0.4ps pulse duration. They also irradiated solids at 45° with p-polarisation. They found a fast electron temperature of 23 keV for irradiances similar to ours. This is a little lower than our temperatures but could be argued to be broadly consistent and might be considered to indicate a similar absorption mechanism. On the other hand, they seem to find laser energy absorption values nearly an order of magnitude lower, for reasons that are at the moment unclear to us. On the other hand Pisani et al [30] used 0.35ps frequency doubled pulses at 529nm, irradiating targets at near normal incidence. They found a fast electron temperature of approximately 175 keV for irradiance of 1-2$\times 10^{18}$Wcm^{-2} which was noted to be in accord with the scaling law given by Beg et al [31], whereas that scaling law would suggest a fast electron temperature of order 100 keV for our case; well above our findings. Since they were working at close to normal incidence with a high contrast laser, it seems likely that an absorption mechanism different

from ours was responsible for the fast electron population.

V. SUMMARY

We have presented data on K-α production that has been used to draw several conclusions. Firstly, we presented data that shows high K-α yield ($> 10^{-4}$) for a pulse wavelength-duration regime that has not been as well explored from this point of view as others. Secondly, in contrast to work at longer pulse durations, we showed that, for this picosecond pulse duration regime, the thermal emission of He-like line radiation is not more efficient than K-α emission; in fact, it is about as efficient as the K-α emission, as was found to be the case for much shorter pulses. Thirdly, we have experimentally demonstrated, unambiguously, the role of electron refluxing even for fast electron temperatures well below 100 keV. Three different assessments of the fast electron temperature were made, one of them direct from hard x-ray measurements, the other two based on simple modelling of fast electron transport and its consequence for K-α yields. These three estimates spanned 30-60 keV but are in broad accord with appropriate scaling laws published in the literature [22, 26–28]. The modelling used for comparison with some of the data is simple but predicts yields in broad agreement with experiment for reasonable estimates of absorption.

Acknowledgments

This work was supported by the UK Engineering and Physical Sciences Research Council (grant numbers EP/C003586/1 and EP/G007462/01)

[1] A. Rousse, P. Audebert, J.P. Geindre, F. Fallies, J.C. Gauthier, A. Mysyrowicz, G. Grillon and A. Antonetti, Phys. Rev. E **5**0, 2200, 1994

[2] C. Reich, P. Gibbon, I. Uschmann and E. Forster, Phys. Rev. Lett **8**4, 4846, 2000

[3] DC Eder, G Pretzler, E Fill, K Eidmann and A Saemann, Appl. Phys B. **7**0, 211-217, 2000

[4] KB Wharton, SP Hatchett, SC Wilks, MH Key, JD Moody, V Yanovsky, AA Offenberger, BA Hammel, MD Perry and C Joshi, Phys. Rev. Lett. **8**1 (4), 822-825, 1998

[5] T. Feurer *et al.*, Phys. Rev. E **6**5, 016412, 2001

[6] D Salzmann, Ch. Reich, I Uschmann, E Frster and P Gibbon, Phys. Rev. E **6**5, 036402, 2002

[7] C. Ziener *et al*, Phys. Rev. E **6**5, 066411, 2002

[8] F Ewald, H Schwaoerer and R Sauerbrey, Europhys. Lett. **6**0, 710-714, 2002

[9] DW Phillion and CJ Hailey, Phys. Rev. A **3**4 (6) 4886-4896, 1986

[10] M.K. Urry, G. Gregori, O.L. Landen, A. Pak and S.H. Glenzer, J. Quantitative Spectrosc. Radiat. Trans. **9**9, 636-648, 2006

[11] LA Gizzi *et al*, Plasma Phys. Contr. Fusion **4**9 B211-B221, 2007

[12] NC Woolsey, D Riley and E Nardi E, Rev. Sci. Instrum. **6**9(2) 418-424, 1998

[13] J Workman and GA Kyrala, Review. Sci. Instr. **7**2(1) 678-681, 2001

[14] D Riley et al, J. Quant. Spectrosc. Radiat. Transfer, **9**9 537-547, 2006

[15] D Riley, NC Woolsey, D McSherry, FY Khattak, and I Weaver, Plasma. Sources. Sci. Technol. **1**1(4) 484-491, 2002

[16] T. Dzelzainis *et al* Laser and Particle Beams, **2**8(3) 451-461, 2010

[17] BR Maddox *et al*, Rev. Sci. Instrum. **8**2 023111, 2011

[18] SM Seltzer, Radiation Research **1**36, 147, 1993

[19] H-K Chung, MH Chen and RW Lee, High Energy Density Physics, **3** 57-64, 2007

[20] WL Kruer *The Physics of Laser Plasma Interactions*, (Westview Press 2003)

[21] P Gibbon and E Förster, Plasma Phys. Contr. Fusion **3**8 769-793, 1996

[22] F Brunel, Phys. Rev. Lett. **5**9 52 1987

[23] D Riley, JJ Angulo-Gareta, FY Khattak, MJ Lamb, PS Foster, EJ Divall, CJ Hooker, AJ Langley, RJ Clarke and D Neely, Phys. Rev. E **7**1(1) art. no. 016406 2005

[24] CA Quarles, Phys. Rev. A **1**3(3) 1278, 1976

[25] P Neumayer *et al*, Physics of Plasmas **1**7, 103103, 2010

[26] DW Forslund, JM Kindel and K Lee, Phys. Rev. Lett. **3**9(5) 284, 1977

[27] SC Wilks and WL Kruer, IEEE Journal of Quantum Electronics, **3**3(11) 1954-1968, 1997

[28] AA Andreev, EG Gamaly , VN Novikov, AN Semakhin and VT Tikhonchuk, Sov. Phys. JETP **7**4 963, 1992

[29] J Yu, Z Jiang and JC Kieffer, Phys. Plasmas **6** 1318, 1999

[30] F Pisani et al, Phys. Rev. E **6**2(5) R5927, 2000

[31] FN Beg, AR Bell, AE Dangor, CN Danson, AP Fews, ME Glinsky, BA Hammel, P Lee, PA Norreys and M Tatarakis, Phys. Plasmas **4**, 447, 1996